Available online at www.sciencedirect.com
ScienceDirect
Journal of Catalysis 254 (2008) 218–225
JOURNAL OF CATALYSIS
www.elsevier.com/locate/jcat

A mechanistic study of the low-temperature conversion of carbon monoxide to carbon dioxide over a cobalt oxide catalyst

Matthew J. Pollard [a], B. André Weinstock [a], Thomas E. Bitterwolf [a], Peter R. Griffiths [a,*], A. Piers Newbery [b], John B. Paine III [b]

[a] *Department of Chemistry, University of Idaho, Moscow, ID 83844-2343, USA*
[b] *New Technology, RD & E, Philip Morris USA, Richmond, VA 23234, USA*

Received 6 July 2007; revised 9 October 2007; accepted 1 January 2008

Available online 7 February 2008

Abstract

A nanocrystalline cobalt oxide (Co_3O_4)-based catalyst formed by heating a basic cobalt(II) carbonate precursor in air at 250–300 °C has been shown to exhibit much greater catalytic activity than Co_3O_4 calcined at higher temperatures. In a highly exothermic reaction, the properly calcined catalyst rapidly oxidizes carbon monoxide to carbon dioxide at room temperature. X-ray diffraction, X-ray photoelectron spectrometry, Brunauer–Emmett–Teller surface area measurements, and two FT-IR techniques were used to investigate the mechanism of the CO oxidation reaction. Diffuse reflection (DR) infrared spectrometry of the catalyst was used to monitor the gases adsorbed on the catalyst surface. The observation of a CO band at 2006 cm^{-1} indicates that CO is adsorbed onto cobalt atoms in a low oxidation state. The highest catalytic activity appears to be achieved when a specific ratio of Co(II) to Co(III) is found on the surface and the particle size is small (i.e., the surface area is large). Poisoning of the catalyst is evidenced in the DR spectra by the geminal adsorption of two CO molecules onto a cobalt atom in a high oxidation state, giving rise to a doublet at ∼2180 cm^{-1}. A strong band at 2343 cm^{-1} indicates that CO_2 is physisorbed onto the catalyst when it is poisoned. A unique ultra-rapid scanning FT-IR spectrometer was used to measure the concentration of the CO_2 formed, as well as that of the unreacted CO within 5 ms after the gas was passed through the catalyst. The spectra indicate that CO_2 is formed in a vibrationally excited state.

Keywords: Cobalt oxide; Low-temperature oxidation; Cabon monoxide; Diffuse reflection; Infrared; Vibrationally excited product

1. Introduction

The exothermic oxidation of carbon monoxide to carbon dioxide over metal oxide catalysts such as Co_3O_4 has been known since the 1920s [1,2]; over the last decade, several studies have revealed details of the reaction. For example, it has been shown that calcination in the presence of oxygen (also described as preoxidation in the literature) yields a highly reactive catalyst for the room-temperature oxidation of carbon monoxide with observed light-off temperatures as low as 210 K [3,4]. These catalytic species are very sensitive to the presence of water that appears to block reactive sites [4,5]. Reaction of CO alone with these catalysts initially yields CO_2, but the rate of this reaction drops quickly, indicating that active surface sites are being depleted. In contrast, mixtures of CO and O_2 maintain good rates of CO oxidation, suggesting that O_2 can replenish the catalytic sites. Furthermore, Jansson showed that when $^{18}O_2$ is used in the calcination step, $C^{16}O^{18}O$ is formed along with negligibly small amounts of $C^{18}O_2$ [6]. It is assumed that ^{18}O either exchanges with surface ^{16}O sites or oxidizes the Co(II) sites that remain after synthesis of the catalyst. Infrared (IR) bands characteristic of carbonate species have been observed on reaction of the cobalt catalysts with CO_2, and CO_2 has been shown to have an inhibitory effect on catalysis. Reaction of $C^{16}O_2$ with an $^{18}O_2$ calcined catalyst gives rise to $C^{16}O^{18}O$, indicating that exchange of surface oxygen with CO_2 can take place [6].

Of particular relevance to the present paper is the fact that several workers have carried out infrared (IR) spectroscopic studies of the catalysts after exposure to CO, CO_2, and mixtures

* Corresponding author.
E-mail address: pgriff@uidaho.edu (P.R. Griffiths).

0021-9517/$ – see front matter
doi:10.1016/j.jcat.2008.01.001

of CO and O_2. For example, Lokhov et al. [7], Goodsel [8], Busca et al. [9], and Lin et al. [10] used Co_3O_4 catalyst materials that had been exposed to high vacuum in the final steps of catalyst preparation. Lokhov et al. [7] also examined the absorption of CO onto Co_3O_4 surfaces at 80 K and observed bands in the infrared spectrum at 2137–2141 and 2125 cm^{-1}. These bands were assigned to metal carbonyl complexes involving Co(III) centers, but we note that free CO trapped in photochemical matrices at the same temperature is known to have stretching frequencies of 2140–2130 cm^{-1}, depending on the matrix environment. Goodsel [8], Busca et al. [9], and Lin et al. [10] have reported carbonyl bands at ca. 2180, 2120, and 2070 cm^{-1} on Co_3O_4 surfaces. At 150 K, the band at 2180 cm^{-1} appeared first, with the other bands appearing as the temperature of the sample was raised to 300 K. Evacuation of the samples led to loss of the two higher-frequency bands. At room temperature and above, bands assigned to carbonate accompanied the appearance of the metal carbonyl bands. Carbonate bands were reported at 1545 and 1324 cm^{-1} by Busca et al. and Goodsel and at 1570 and 1333–1302 cm^{-1} regions by Lin et al. These bands did not exactly match the expected positions for free carbonate (1440 cm^{-1}), unidentate carbonate (1470–1450, 1380–1350, 1070–1050 cm^{-1}), or bidentate carbonate (1640–1590, 1290–1260, 1040–1020 cm^{-1}) and are presumably caused by breaking of the trigonal symmetry of free carbonate ions. The bands reported by Busca et al., Goodsel, and Lin et al. stand in sharp contrast to bands at ca. 1605, 1420, and 1220 cm^{-1} on preoxidized Co_3O_4 reported by Jansson et al. [11,12]. A pair of bands at 2155 and 2178 cm^{-1} that were assigned to cobalt carbonyl groups also was observed by Jansson et al.

A group of bands at 1300–990 cm^{-1} was assigned by Jansson to a surface O_2^{n-} species involving O_2 reactions with iron surfaces by analogy to earlier work of Al Mashta et al. [13]. These low-frequency bands, which were assigned to harmonics of skeletal bands, also were reported in the spectra of evacuated samples by Busca et al. Because these bands were observed in samples that had been heated to remove a nonstoichiometric excess of oxygen, Jansson's assignment of the bands at 1640–1200 cm^{-1} to cobalt carbonyl groups appears to be incorrect.

Finally, we note the work of Todorova et al. [14], who prepared cobalt oxide catalysts on alumina by the thermal decomposition of $Co(NO_3)_3$. Heating these materials to 573 K in a stream of hydrogen followed by exposure of the catalyst to CO resulted in the appearance of a band at 2170 cm^{-1} similar to the high-frequency bands noted above. When these catalysts were reduced by heating to 723 K in a stream of hydrogen and then exposed to CO, a new band at 2005 cm^{-1} was observed.

In this paper, we report the results of our investigation of the reaction mechanism of the room-temperature oxidation of carbon monoxide to carbon dioxide over a cobalt catalyst prepared by the calcination of basic cobalt(II) carbonate at temperatures significantly below 500 °C. When basic $CoCO_3$ is calcined in air at ∼250 °C, it is largely decomposed to the oxide, and the Co(II) is partially oxidized to Co(III), to form what is nominally "Co_3O_4" but which shows signs of retaining some of its original carbonate content (see below), compared with samples prepared by calcination at much higher temperatures.

2. Experimental

2.1. Catalyst preparation

Basic $CoCO_3$ was synthesized by dissolving cobalt(II) nitrate hexahydrate ($Co(NO_3)_2{\cdot}6H_2O$) in water and subsequent acidification with concentrated nitric acid (Ref. [15], Example 15). This solution was then added dropwise over several hours to a stirred solution of excess sodium carbonate. The resulting precipitate was vacuum-filtered and thoroughly washed with distilled water. The washed precipitate was dried at 110 °C in ambient air for 12 h to produce the basic $CoCO_3$ catalyst precursor. This catalyst precursor was crushed and sieved to form a fine powder, which was then heated in a tube furnace at ca. 250 °C with flowing nitrogen and 21% oxygen at a rate of 200 mL/min to form the cobalt oxide catalyst.

2.2. Catalyst characterization

The catalyst formation was investigated using thermogravimetric analysis (TGA) (Netzsch STA49PC). Approximately 5 mg of 20- to 40-mesh basic cobalt carbonate was placed in an aluminum sample pan. The catalyst was then calcined *in situ* by heating it to 250 °C at 20 °C/min, holding at this temperature for 1 h, and then cooling it to 30 °C, under a flow of 21% oxygen in helium (BOC Gases) at 200 mL/min. The weight loss of the sample was recorded during calcination. After calcination, the gas was switched to a carbon monoxide and oxygen mixture in helium (3.4% CO, 10% O_2 and 86.6% He; BOC Gases), again at 200 mL/min. This mixture was flowed over the catalyst for 2 h, during which time the heat generated by the exothermic reaction was recorded by differential scanning calorimetry (DSC). Values of the exotherm were recorded after 10 min of exposure and again after 2 h.

Elemental ratios of carbon, oxygen, and cobalt and the ratio of Co(II) to Co(III) in the catalyst were determined using X-ray photoelectron spectrometry (XPS). In this procedure, 50-mg samples of 20- to 40-mesh basic cobalt carbonate were calcined for 1 h at 200, 250, 300, or 400 °C. Subsamples of the calcined catalyst and the basic cobalt carbonate were pressed into indium and then loaded into a 10^{-9} Torr vacuum chamber for examination with a Kratos Axis 165 XPS (15 mA, 13,500 kV, MgK_α radiation source, 3-mm^2 focal point area, 0.8-eV resolution). Survey scans (0–1000 eV) were performed for determination of purity and elemental ratios, and detailed scans in the 770–815 eV region were run to determine the Co(II):Co(III) ratio using the cobalt $2p_{3/2}$ and $2p_{1/2}$ electron emission peaks. Gaussian peak fitting was performed using Shirley baseline correction.

The catalyst surface area was measured with a 5-point BET analysis with nitrogen at 77.4 K using a Quantachrome AUTOSORB-1 analyzer. Powder X-ray diffraction (XRD) patterns were obtained with a Philips X'Pert system (45 kV, 40 mA, CuK_α radiation source).

2.3. Diffuse reflectance FT-IR measurements of the catalyst

The calcination process, adsorption of CO and poisoning of the catalyst were all monitored *in situ* using a custom-built diffuse reflectance accessory that allowed higher optical throughput than any commercially available apparatus [16]. The collimated infrared beam from the interferometer of an ABB Bomem MB-100 FT-IR spectrometer was passed through the external beam port of the spectrometer and translated through 2-plane periscope mirrors onto a 45-degree off-axis paraboloidal mirror that focused the collimated IR beam from the interferometer onto the sample. A portion of the diffusely reflected beam from the sample was then collected by one half of a large paraboloidal mirror and focused onto a downward-looking mercury cadmium telluride (MCT) detector by the other half of this mirror. The data acquisition time for the spectra shown herein was about 6 min. The sample holder was both heatable and evacuable, with the gas in the body of the cell being drawn through the powdered sample by a vacuum pump. The sample cup held approximately 0.17 mL of sample on a 50-μm screen. The window of the sample cell was a 50-mm-diameter CaF_2 disk. The temperature of the catalyst was monitored throughout the calcination, CO adsorption, CO_2 evolution, and deactivation process.

Neat basic $CoCO_3$ was heated *in situ* in the presence of air for 1 h at 250 °C. DR spectra of the sample were measured during this calcination process. After 1 h, the sample was evacuated and cooled rapidly to 15 °C. At this point, the sample was considered activated and suitable as a catalyst for CO oxidation. CO gas (Matheson, 99.9%) was introduced to the system by flowing it slowly through the catalyst.

2.4. Ultra-rapid scanning FT-IR spectrometry of the gaseous products

In a separate series of measurements, a unique ultra-rapid scanning FT-IR spectrometer that can measure spectra between 4000 and 900 cm^{-1} at a resolution of 6 cm^{-1} at 5-ms intervals [17–21] was used to monitor the gaseous CO_2 formed by oxidation of the carbon monoxide that flows through the catalyst along with any unreacted CO. The apparatus has been described previously [19–21], and only significant aspects of it are discussed here. The gas mixture produced in a 12-L glass bulb was passed through the sample for up to 5 s through a solenoid valve that could be opened or closed in ∼1 ms. The catalyst sample was held on a 20-μm mesh stainless steel screen epoxied into a $\frac{1}{4}$-inch (∼6 mm)-i.d. Swagelok elbow union. The gas that passed through the catalyst and screen entered a 20-reflection, 2.4-m path-length cell with a volume of ∼125 mL (Infrared Analysis, Anaheim, CA).

Then 0.050 g of neat basic $CoCO_3$ was heated for 1 h at 250 °C in an unsealed oven. While still hot, the catalyst was quickly transferred to the sample holder. Before injection of the CO, the sample was evacuated to a pressure <1 mTorr.

Various gas mixtures of CO with N_2, O_2, ambient air, or H_2O-free, CO_2-free air were prepared to a total pressure of 200.0 Torr in the 12-L bulb. A portion of the gas mixture was then injected by the solenoid valve through the activated catalyst and into the multipass IR gas cell. The solenoid valve was opened for 1.5–5.0 s; spectra were measured every 5 ms for the first 1.5 s of the injection using the ultra-rapid scanning FT-IR spectrometer. Further spectra were obtained at 1, 2, 5, 10, 20, and 30 min after the injection.

The reference spectrum of CO_2 in the ground vibrational state was obtained by calculating the ratio of the single-beam spectrum measured with ambient air in the cell to that of the evacuated IR multipass cell.

3. Results and discussion

3.1. Catalyst characterization

3.1.1. Powder X-ray diffraction

XRD traces of the calcined cobalt basic carbonate contained peaks belonging to the Co_3O_4 spinel phase, although the peaks were low in intensity and broad compared with commercially prepared Co_3O_4. For the cobalt oxide calcined at 175 °C, only the peak at $2\theta = 37°$ could be distinguished, as shown in Fig. 1. As the calcination temperature was increased to 500 °C, the intensity of the weaker peaks increased and the width of the peak at $2\theta = 37°$ decreased. The increasing definition of many of the peaks was due to an increase in crystallite size, which accounts for the decrease in surface area at higher temperatures. Additional contributions to the change in surface area were made by the increasing development of the Co_3O_4 spinel crystal structure at the expense of the amorphous structure of the basic carbonate, and by the initially formed amorphous oxides.

3.1.2. X-ray photoelectron spectrometry

XPS survey scans and detailed scans of the cobalt $2p_{3/2}$ and $2p_{1/2}$ electron emission peaks showed no variance in the elemental composition and oxidation state of the catalyst calcined

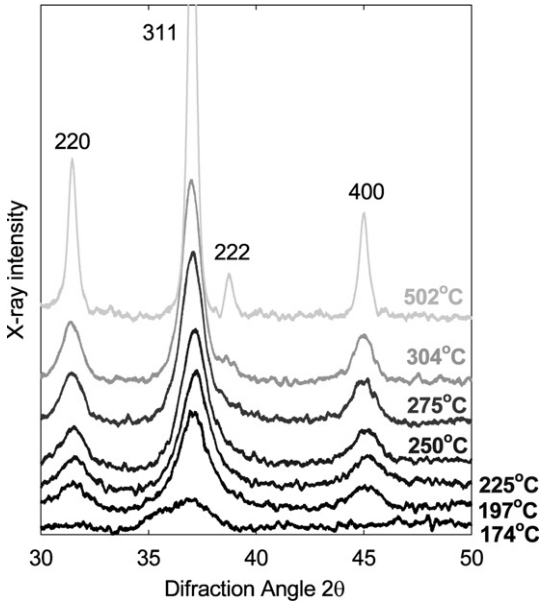

Fig. 1. Powder XRD traces of cobalt oxide formed during a 21% O_2 in N_2 calcination cycle. The assigned peaks are from the Co_3O_4 spinel structure.

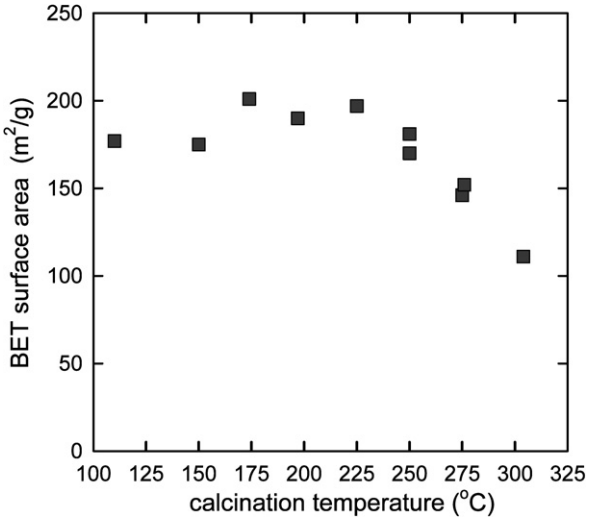

Fig. 2. BET surface area of the cobalt oxide formed during a 21% O_2 in N_2 calcination as a function of calcination temperature.

at 200–400 °C. Spectra of the basic cobalt catalyst precursor show that it was thermally dehydrated under high vacuum and composed of the stoichiometric ratio $CoCO_3$ with all of the cobalt atoms in the Co(II) state. The calcined samples retained a considerable amount of $CoCO_3$ (occupying about a quarter of the surface cobalt sites), with the remainder of the sample consisting of a mixed-valent cobalt oxide. The $2p_{3/2}$ electron emission peak showed a shift characteristic of an entirely Co(II) surface composition for the basic cobalt carbonate to a mixed valence composition with a ratio of approximately one Co(II) to four Co(III) sites for the calcined catalyst samples. The XPS finding of a Co(II):Co(III) ratio of 1:4 on the catalyst surface (well beyond the 1:2 ratio of Co_3O_4) may reflect the high surface area of this material relative to that of crystalline Co_3O_4.

3.1.3. BET surface area analysis

The BET surface area of the dried cobalt basic carbonate before calcination was ∼175 m^2/g. The surface area of the cobalt oxide catalyst was dependent on the temperature of calcination. As shown in Fig. 2, as the calcination temperature was increased up to 200 °C, the surface area increased to ∼200 m^2/g, and at temperatures above 225 °C, the surface area decreased steadily with increasing temperature, reaching 111 m^2/g at 300 °C and 32 m^2/g by 500 °C. These results, along with the DSC, TGA, and XRD data, suggest that the surface area decreased as the calcination temperature was increased above 300 °C, consistent with the growth of crystallites of the spinel phase of Co_3O_4. It should be noted that Busca et al. [9] and Goodsel [8] reported surface area values for their catalytic samples of 15 and 25–30 m^2/g, respectively.

3.1.4. Differential scanning calorimetry

Because the reaction was so highly exothermic, obtaining highly reproducible results by DSC was difficult. (In one of the diffuse reflection FT-IR measurements, so much heat was generated that the stainless steel mesh on which the catalyst was mounted melted when a mixture of air and CO_2 was passed slowly through it.) The most active catalysts were obtained when the basic $CoCO_3$ was calcined at 175–250 °C. Catalytic activity remained fairly constant when the calcination temperature was further increased to 300 °C. At higher calcination temperatures (∼500 °C), the catalytic activity decreased. DR/IR spectrometry demonstrated that the weight loss of 17–25% found at calcination temperatures of 175–250 °C is due largely to dehydration and decarboxylation of the hydroxide and carbonate groups of the basic $CoCO_3$. The activity of the catalyst decreased slightly when it was exposed to a mixture of CO and O_2 (3.3% CO and 21% O_2 in helium) for longer than a few minutes. The temperature of the catalyst can increase by as much as 50 °C during CO exposure and subsequent CO_2 evolution.

When the catalyst was heated in an inert rather than an oxygen-rich atmosphere, very little catalytic activity was seen, and the sharp peak in the DSC trace caused by CO oxidation was strongly reduced in magnitude.

3.1.5. Diffuse reflection infrared spectroscopy

Before the catalyst precursor was heated, its DR spectrum was dominated by the antisymmetric C–O stretching band of CO_3^{2-} (1600–1300 cm^{-1}) and the very broad O–H stretching band of OH^- or adsorbed water (3700–3300 cm^{-1}). After calcination of the precursor at 250 °C for 5 min, these bands were considerably weaker, although the carbonate bands did not disappear completely, as can be seen in Fig. 3. The strongest band in the spectrum of free CO_3^{2-} ions is usually seen at 1440 cm^{-1}. With a loss of CO_2 from the precursor, two bands at 1510 and 1340 cm^{-1} appeared, at frequencies similar to those reported by Goodsel [8] and Busca et al. [9], indicating a reduction in the trigonal symmetry of free carbonate ions. (Free carbonates also have another, sharper and weaker, band that absorbs at ∼850 cm^{-1}, but this is below the cutoff of the CaF_2 window of our cell.)

The XRD analysis also suggests that whereas the catalysts used in this work contained characteristic peaks of spinel Co_3O_4, those bands were relatively broad, suggesting that this phase composed only a portion of the sample. Thus, it is reasonable to assume that the catalyst formed by the calcination of basic $CoCO_3$ under our conditions was not the same as the pure Co_3O_4 catalyst investigated by previous workers, but instead was an ill-defined mixture of Co_3O_4 (not necessarily all crystalline), CoO, and "$CoCO_3$," or related carbonate.

In addition to the carbonate bands described above, exposure of the Co_3O_4 catalyst to CO resulted in the appearance of bands at 2200–2000 cm^{-1} region characterized as metal carbonyl or weakly physisorbed CO. In the present work, bands were observed centered at 2006 cm^{-1} and as a doublet at 2172 and 2189 cm^{-1}.

The assignment of carbonyl bands to specific metal oxidation state/carbonyl interactions is complicated by the lack of well-defined high-oxidation state reference compounds. A relatively small number of organometallic compounds feature Co in the +3 formal oxidation state; examples of such compounds include $CpCo(CO)I_2$ (ν_{CO} = 2045 cm^{-1}) [22], $Cp^*Co(CO)(Cl(CH_2Cl)$ (ν_{CO} = 2030 cm^{-1}) [23], and

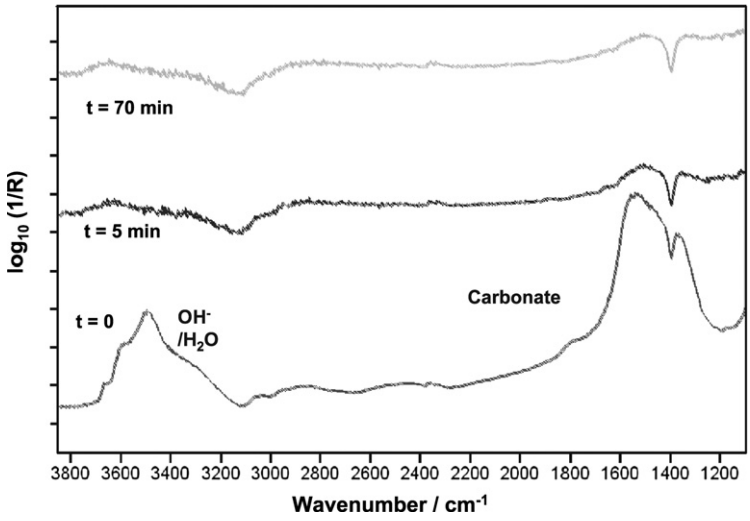

Fig. 3. Diffuse reflection spectra measured during calcination of basic $CoCO_3$ vs a spectrum of powdered KBr. The lowest spectrum is that of basic $CoCO_3$ prior to calcination with the upper spectra measured after calcination for 5 and 70 min.

$CpCo(CO)(CF_3)_2$ ($\nu_{CO} = 2083\ cm^{-1}$) [24]. Some porphyrin cobalt carbonyl complexes are known that come closer to the hard ligand environment of a metal oxide. Cobalt(II) porphyrin derivatives have been studied in frozen gas matrices, Co(TPP))CO ($\nu_{CO} = 2077\ cm^{-1}$) and $Co(TPP)(CO)_2$ ($\nu_{CO} = 2073\ cm^{-1}$) [25], and cobalt(III) derivatives, $[Co(OEP)(CO)]ClO_4$ ($\nu_{CO} = 2110\ cm^{-1}$) and $[Co(OEP)(CO)_2]ClO_4$ ($\nu_{CO} = 2137\ cm^{-1}$), have been examined by both solution IR and Raman spectroscopy [26]. It is very reasonable to expect CO bound to a Co(II) or Co(III) in an oxide matrix to have carbonyl stretching bands at higher frequency than the porphyrin compounds. Thus, it appears reasonable to assign the bands with frequencies above that of gas-phase CO (i.e., with $\nu_{CO} > 2145\ cm^{-1}$) to CO bonded to Co(III).

The cobalt oxide catalyst examined in this study was shown to bind carbon monoxide in two very different environments, indicated by a pair of bands ca. 2180 cm^{-1} and a broad singlet centered at 2006 cm^{-1}. High-frequency carbonyl bands have been reported by several groups and are consistent with carbonyl binding to Co(III) in the spinel Co_3O_4 phase; for example, based on earlier assignments by Merbler et al. [27], Jansson et al. [6,11,12] assigned high-frequency carbonyl bands to CO groups bound to Co(III) sites in the catalyst. The carbonyl band at 2006 cm^{-1} has precedence in the work of Todorova et al. [14], who found similar bands in cobalt oxide catalysts that had been reduced with H_2. In the present work, the band at 2006-cm^{-1} arose during the oxidation cycle and may correspond to carbon monoxide bound to cobalt atoms that have undergone one oxidation cycle and been reduced from Co(III) to a lower oxidation state.

The observed IR behavior of the sample in the presence of CO is consistent with some of the mechanistic hypotheses presented above. The relatively weak band at 2006 cm^{-1} almost certainly should be assigned to CO linearly adsorbed on Co(II). The intensity of this band increased slowly with the amount of time that gaseous CO was passed through the catalyst; see Fig. 4. We did not observe this band when mixtures of oxygen and CO were passed through the catalyst, demonstrating the short lifetime of the adsorbed CO when conditions are appropriate for its rapid oxidation.

After 20 min, the flow of CO was terminated and the system evacuated. After a second calcination cycle (in air), the catalyst was exposed to CO just as was done in the initial process. Even though the intensity of the CO_3^{2-} bands was somewhat reduced during this second calcination step, the second CO oxidation cycle usually yielded similar spectra to the first one, with the intensity of the bands due to adsorbed CO being approximately the same as in the initial cycle.

During one experiment in which the calcination temperature was believed to be higher than usual, some very unusual differences were observed. The spectra obtained in this experiment are shown in Fig. 5. The large, rapid increase in the intensity of the carbonate bands indicates that a significant proportion of the CO_2 formed when the surface was first exposed to CO reacted to form carbonate ions. The band at 2006 cm^{-1} assigned to CO linearly bonded on Co(II) is missing from this spectrum, but three new bands can be seen at 2172, 2189, and 2343 cm^{-1}. The 2343-cm^{-1} band can be readily assigned to physically adsorbed CO_2. The absence of the P and R branches in the typical vibration-rotation contour of CO_2 indicates that this band definitely was not due to CO_2 in the gas phase. The finding that not all of the CO_2 formed was swept through the catalyst, but some was adsorbed onto its surface, implies that the catalyst became deactivated, as indicated by its relatively low temperature. This type of adsorption is speculated to indicate catalyst poisoning.

The assignment of the 2172- and 2189-cm^{-1} bands is less straightforward. We believe that they are probably best assigned to the symmetric and antisymmetric stretching modes of CO that is geminally disubstituted on a cobalt atom in a high oxidation state. Most bands due to adsorbed CO absorb at a lower wavenumber than gaseous CO (for which the fundamental vibrational frequency is 2145 cm^{-1}), but several examples of CO absorbing at a wavenumber greater than the fundamental frequency of CO (~2145 cm^{-1}) have been reported. Janssen [6]

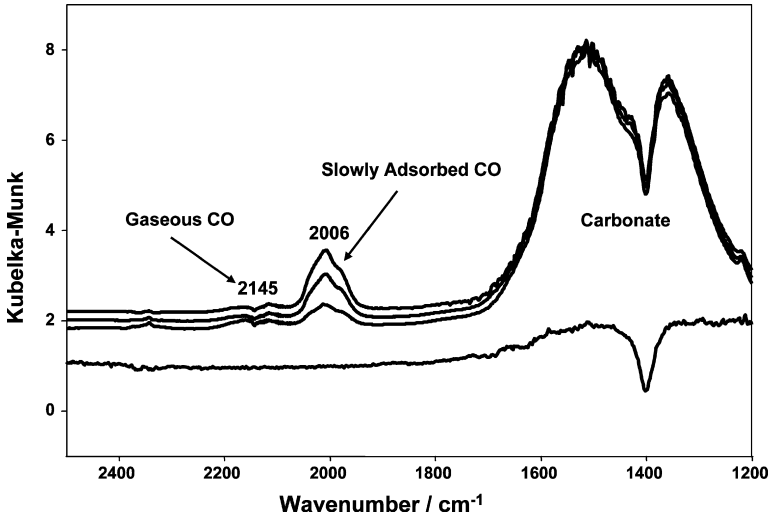

Fig. 4. DR spectra measured while CO is flowing through the activated catalyst; spectra were ratioed against spectra of powdered KBr. The lowest spectrum is that of the calcined $CoCO_3$ prior to exposure to CO. The upper spectra were measured immediately after exposure to flowing pure CO gas and 10 and 20 min after exposure.

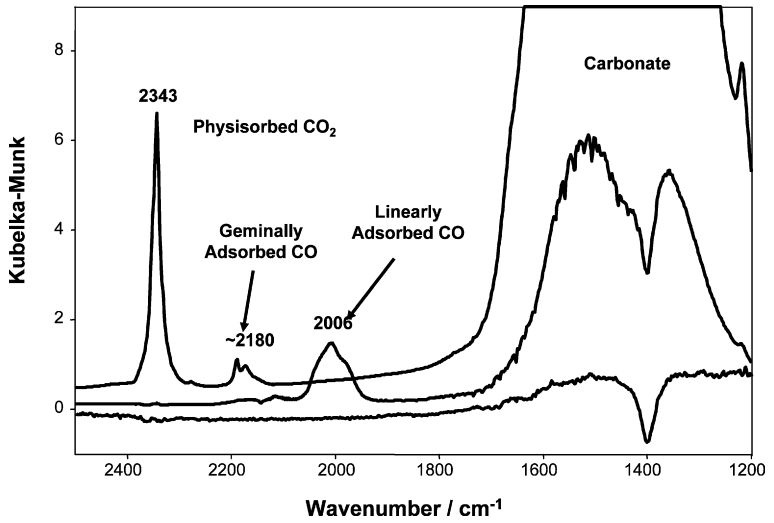

Fig. 5. DR spectra measured while CO is flowing through the activated catalyst during two oxidation cycles (versus KBr). The lower spectrum is the calcined catalyst after one oxidation cycle.

has reported frequencies of CO adsorbed onto cobalt atoms in different oxidation states as 2023–2025 cm^{-1} for Co(0), 2070–2110 for Co(I), 2120–2170 cm^{-1} for Co(II), and 2178–2180 cm^{-1} for Co(III). We have some doubts about the spectral ranges for the stretching mode of CO adsorbed on low-valent cobalt, because we found a band at 2006 cm^{-1} that is probably best assigned to CO adsorbed on Co(II) and is below the lowest frequency reported by Janssen. Nonetheless, the frequencies of the doublet that we observed are in the correct range for CO adsorbed on Co(III), because it is well known that if the frequency of any metal carbonyl is greater than that of free CO (2145 cm^{-1}), then the oxidation state of the metal must be very high.

Before performing the XPS study, we believed that the changes in catalytic activity with increasing calcination temperature were best explained by an increase in the number of Co(III) atoms—along with a concomitant decrease in the number of Co(II) atoms—on the surface as the calcination temperature is increased. It seemed logical that for the reaction to occur at its highest efficiency, the number of Co(II) and Co(III) atoms adjacent to each other should be at some optimal value (e.g., 1:1). In fact, the XPS data revealed a Co(II):Co(III) ratio of approximately 1:4 for catalysts produced by calcination at all temperatures between 200 and 400 °C. The catalytic activity decreased by about 20% as the calcination temperature was increased from 200 to 300 °C. This result seems surprising; we expected the concentration of Co(III) sites to increase continuously with increasing calcination temperature. As noted above, however, XPS showed that the Co(III):Co(II) ratio was approximately constant for calcination temperatures of 200–400 °C. On the other hand, BET measurements showed that the surface area decreased with calcination temperature, and XRD demonstrated that the crystallite size increased with calcination temperature. Thus, it is logical to conclude that the highest

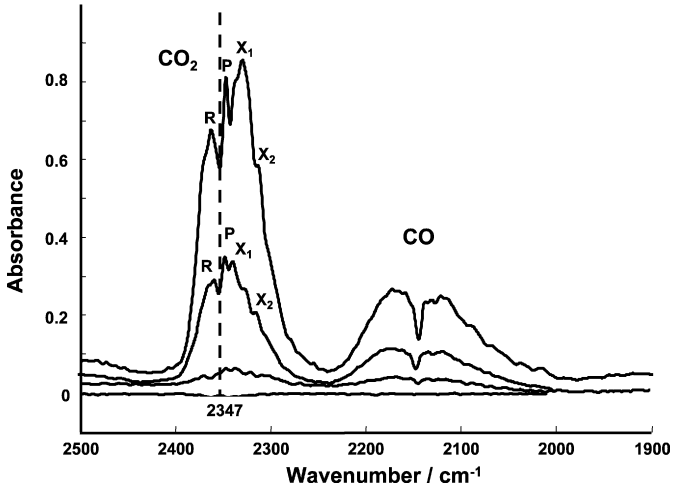

Fig. 6. Spectra of CO_2 and CO measured 1.00 second after injection of a mixture of 10.0 Torr of CO and 189.6 Torr of N_2 through ∼0.04 g of the catalyst that had been activated at 250 °C for 1 h.

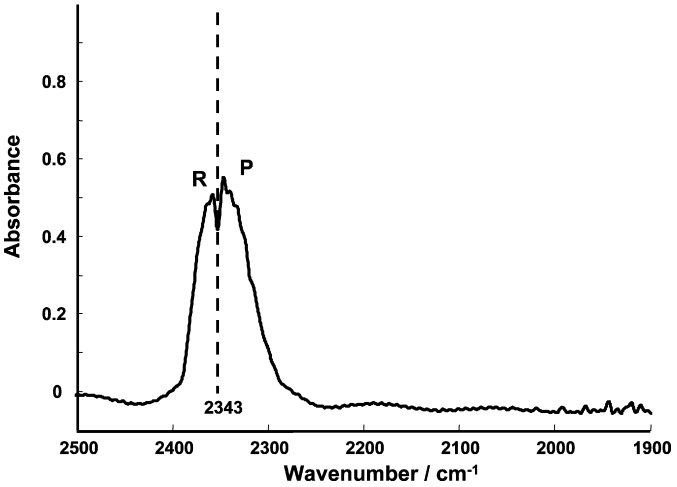

Fig. 7. Reference spectrum of ambient CO_2 measured on the same spectrometer under identical conditions as seen in Fig. 6.

efficiency occurs when the particle size is as small as possible.

3.1.6. Ultra-rapid scanning FT-IR spectrometry

Time-resolved spectra of carbon dioxide produced by the catalyst are shown in Fig. 6. For comparison, a spectrum of CO_2 at ambient pressure and temperature is shown in Fig. 7. When the infrared spectrum of CO_2 in air at ambient temperature was measured at a resolution of 6 cm^{-1} the rotational lines were not resolved, but a dip between the P and R branches was still seen at the fundamental vibrational frequency of the ν_3 band of CO_2 (∼2347 cm^{-1}). Under ambient conditions, the integrated area of the P branch was approximately the same as that of the R branch.

Fig. 6 shows three spectra obtained at 100, 250, and 550 ms into a 500-ms exposure of the catalyst to a mixture of 133 Torr CO and 67 Torr O_2. Because a small fraction of the catalyst was blown through the frit into the IR gas cell, production of CO_2 continued even after the solenoid valve was closed. The production of CO_2 in the ground vibrational state, identified by the P and R branches centered around ∼2347 cm^{-1}, and the appearance of excess CO, centered at ∼2145 cm^{-1}, are apparent. For comparison, Fig. 6 also shows a spectrum obtained 10 ms before the exposure of CO and O_2.

Of particular interest are the features seen below 2347 cm^{-1} (labeled X_1 and X_2), assigned to transitions between vibrationally excited states of the antisymmetric stretching mode (ν_3) of CO_2 ("hot bands"). These hot bands were centered below the fundamental due to the effect of anharmonicity. The integrated absorbance of the bands below 2347 cm^{-1} was significantly greater than the integrated absorbance of the band above 2347 cm^{-1}. Similar effects were not seen in the spectrum of CO that passed through the catalyst unreacted, demonstrating that only the CO_2 in the gas cell was vibrationally excited. Unfortunately, we could not detect similar effects in the ν_2 (bending) mode, because it absorbed below the cutoff of our photoconductive MCT detector. A non-Boltzmann distribution of the vibrational states of catalytically produced gas molecules has been studied by Molinari [28], leading us to conclude that we were in fact producing CO_2 for which the ν_3 band is vibrationally excited. The mechanism of production of the vibrationally excited CO_2 from the heterogeneous catalyst is currently unknown; we propose a possible mechanism. The highly exothermic nature of the catalytic reaction during the oxidation process almost certainly plays a role in the excitation. It may be that involvement of peroxide oxygen or superoxide oxygen in the mechanism provides a sufficient excess of energy to provide excited carbon dioxide as a product. Further experiments should be performed in an attempt to fully match Molinari's theory and our observations.

4. Conclusion

Our findings provide some insight into the mechanism of the oxidation of CO to CO_2. Fig. 8 illustrates our proposed mechanism. CO is adsorbed on Co atoms in a low oxidation state, presumably Co(II). The adsorbed CO interacts with an oxygen atom bonded to a neighboring Co(III) atom in a strongly exothermic reaction, forming vibrationally excited CO_2. The oxygen atom that was lost is then replaced by oxygen present in the input gas, thereby reoxidizing this cobalt atom. CO can be adsorbed on a neighboring Co(II) site, in which case the catalytic cycle is maintained. If the Co(III) site is blocked by the adsorption of one or more CO molecules or by CO_2 formed in the reaction, then the catalyst is poisoned.

In summary, therefore, the combination of DSC, TGA, XRD, XPS, BET isotherms, DR/FT-IR spectrometry of the catalyst, and very rapid FT-IR measurements of the gaseous products have provided significant information on the mechanism of the catalytic oxidation of CO to CO_2 on a mixed-valence cobalt catalyst.

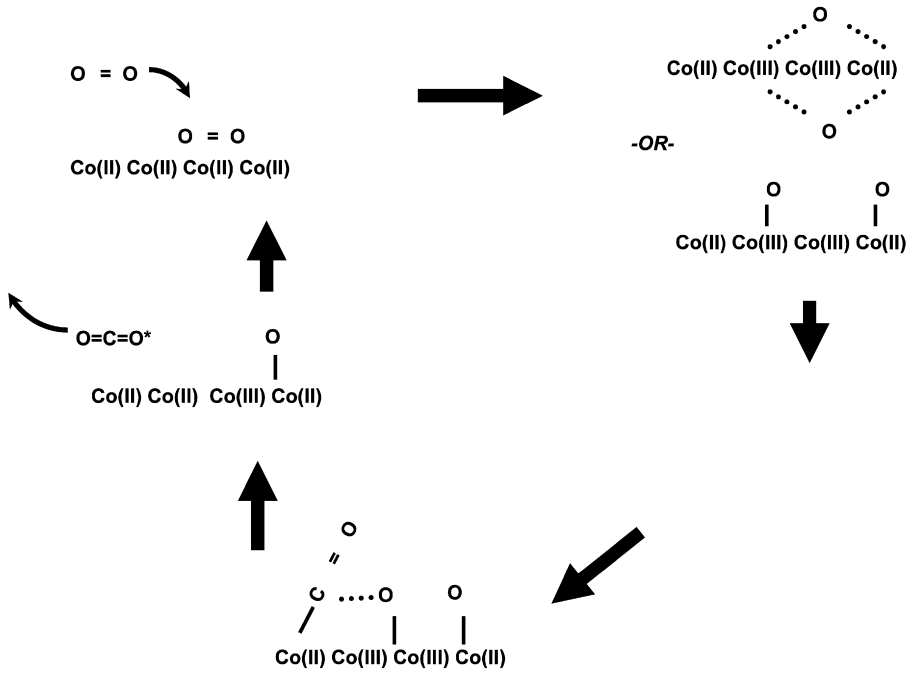

Fig. 8. Proposed mechanism. See text for description.

Acknowledgments

The authors thank Dr. Louis Scudiero, Department of Chemistry, Washington State University, for help with the XPS data collection and interpretation.

References

[1] B.L. Yang, S.F. Chan, W.S. Chang, Y.Z. Chen, J. Catal. 130 (1991) 52–61.
[2] D.R. Merrill, C.C. Scalione, J. Am. Chem. Soc. 43 (1921) 1982.
[3] P. Thormählen, M. Skoglundh, E. Fridell, B. Andersson, J. Catal. 188 (1999) 300–310.
[4] D.A.H. Cunningham, T. Kobayashi, N.K. Haruta, M. Haruta, Catal. Lett. 25 (1994) 257–264.
[5] P. Thormählen, E. Fridell, N. Cruise, M. Skoglundh, Appl. Catal. B 31 (2001) 1–12.
[6] J. Jansson, J. Catal. 194 (2000) 55–60.
[7] Yu.A. Lokhov, S.F. Tikhov, M.N. Bredikhin, A.G. Zhirnyagin, V.A. Sadykov, Mendeleev Commun. (1992) 10–11.
[8] A.J. Goodsel, J. Catal. 30 (1973) 175–186.
[9] G. Busca, R. Guidetti, V. Lorenzelli, J. Chem. Soc. Faraday Trans. 86 (1990) 989–994.
[10] H.-K. Lin, C.-B. Wang, H.-C. Chiu, S.-H. Chien, Catal. Lett. 86 (2003) 63–68.
[11] J. Jansson, M. Skoglundh, E. Fridell, P. Thormählen, Top. Catal. 16/17 (1–4) (2001) 385–389.
[12] J. Jansson, A.E.C. Palmqvist, E. Fridell, M. Skoglundh, L. Österlund, P. Thormählen, V. Langer, J. Catal. 211 (2002) 387–397.
[13] F. Al Mashta, N. Sheppard, V. Lorenzelli, G. Busca, Faraday Trans. I 78 (1982) 979–989.
[14] S. Todorova, V. Zholyazkov, G. Kadinov, React. Kinet. Catal. Lett. 57 (1996) 105–110.
[15] R.L. Augustine, J.A. Fournier, J.B. Paine III, K.H. Shafer, S.K. Tanielyan, US Pat. 5,502,019, Mar. 26, 1996.
[16] I.M. Hamadeh, D. King, P.R. Griffiths, J. Catal. 88 (1984) 264–272.
[17] P.R. Griffiths, B.L. Hirsche, C.J. Manning, Vib. Spectrosc. 19 (1999) 165–176.
[18] C.J. Manning, US Pat. 5 898 495, Apr. 27, 1999.
[19] B.A. Weinstock, H. Yang, P.R. Griffiths, Vib. Spectrosc. 35 (2004) 145–152.
[20] B.A. Weinstock, H. Yang, B.L. Hirsche II, P.R. Griffiths, Langmuir 21 (2005) 3915–3920.
[21] H. Yang, B.A. Weinstock, B.L. Hirsche II, P.R. Griffiths, Langmuir 21 (2005) 3921–3925.
[22] B.B. King, Inorg. Chem. 5 (1966) 82–87.
[23] W.L. Olson, D.A. Nagaki, L.F. Dahl, Organometallic 5 (1986) 630–634.
[24] C.D. Ontiveros, J.A. Morrison, Organometallics 5 (1986) 1446–1448.
[25] M. Kozuka, K. Nakamoto, J. Am. Chem. Soc. 103 (1981) 2162–2168.
[26] E. Schmidt, H. Zhang, C.K. Chang, G.T. Babcock, W.A. Oertling, J. Am. Chem. Soc. 118 (1996) 2954–2961.
[27] Y.J. Mergler, A. van Aalst, J. van Delft, B.E. Nieuwenhuys, J. Catal. 161 (1996) 310–318.
[28] E. Molinari, M. Tomellini, Catal. Lett. 83 (2002) 71–78.